SPE 118879

History matching using a hierarchical stochastic model with the ensemble Kalman filter: a field case study

Yanfen Zhang, Dean S. Oliver, SPE, University of Oklahoma

This paper was prepared for presentation at the 2009 SPE Reservoir Simulation Symposium held in Houston, Texas, U.S.A., 2-4 February 2009.

Abstract

The growth in the application of optimization in reservoir management has placed greater demands on the application of history matching to produce models that not only reproduce the historical production behavior, but also preserve geological realism and quantify forecast uncertainty. Geological complexity and limited access to the subsurface typically result in a large uncertainty in reservoir properties and forecasts. There is, however, a systematic tendency to underestimate such uncertainty, especially when rock properties are modeled using Gaussian random fields. In this paper, we address two sources of uncertainty: uncertainty in regional trends by introducing stochastic trend coefficients and uncertainty in variogram model by treating correlation length or range as a stochastic variable instead of a well-determined variogram parameter. The hierarchical parameters including trend coefficients and heterogeneities can be estimated using ensemble Kalman filter (EnKF) for history matching.

Hierarchical or multi-scale heterogeneities are generally poorly represented, especially in deepwater reservoirs. We developed a hierarchical description of heterogeneities that introduced new variables into the reservoir description. We tested our method for updating these variables using production data from a deepwater field whose reservoir model has over 200,000 unknown parameters. The match of reservoir simulator forecasts to real field data using a standard application of EnKF had not been entirely satisfactory, as it was difficult to match water cut in one of the wells. None of the realizations of the reservoir exhibited water breakthrough using the standard method. By adding uncertainty in trends of reservoir properties, the ability to match the water cut and other production data was improved substantially.

The results indicate that an improvement in the generation of the initial ensemble and in the variables describing the property fields give an improved history match with plausible geology. It reduces the tendency to underestimate uncertainty while still providing reservoir models that match data.

Introduction

Uncertainty underestimation problem There is an almost universal tendency for people to underestimate uncertainty, which is a result of lack of complete knowledge of the factors contributing to the uncertainty. In some cases, even though the factors contributing to uncertainty are known, there is no practical way to quantify the uncertainty. Many projects end up costing much more than the initial estimates. Such cost underestimation has a long history due to lack of adequate uncertainty quantification (Capen 1976). In the petroleum industry, advances in seismic technology have improved our ability to image the reservoir architecture, but seismic technology alone is incapable of determining flow properties and small-scale features needed for reservoir models. Moreover, different geological processes can result in significant variation in reservoir facies distribution and petrophysical properties. In addition, optimal sampling and observations are always limited (Yang et al. 2000). As a result, a high degree of uncertainty exists when building reservoir models, especially if the reservoir lies in a complex deepwater channel systems. Stochastic modeling is useful because it provides a systematic way of quantifying uncertainty by generating multiple reservoir property models. There is, however, a systematic tendency to underestimate such uncertainty, especially when rock properties are modeled using Gaussian random fields (Oliver et al. 2008). In Gaussian simulation, it is common to either assume second-order stationarity of the random field, or that the trend (or drift) is known and the heterogeneity (or residuals) are stationary (Deutsch 2002). But the fact is that there are always trends existing in the geological properties, they just appear different under different measuring scales. In this work, we quantify the underestimated uncertain from two sources. First, we address the uncertainty in regional trends by introducing stochastic trend coefficients in a polynomial trend model. Second, we quantify the uncertainty in the variogram model by treating the correlation length, which controls the range over which heterogeneities are correlated in a region, as a random variable with specified prior distribution. The hierarchical parameters including trend coefficients and heterogeneities can be estimated using ensemble Kalman filter (EnKF) for history matching.

EnKF as a history matching method EnKF is an efficient assisted history matching method which has attracted increasing attention in petroleum industry in recent years. The features that make EnKF attractive and useful in many different contexts are briefly summarized here:

- The correlations between model variables and theoretical data are estimated based only on the information from the ensemble. Thus EnKF is independent of the simulator, and it can be coupled with any reservoir simulator without adjoint codes.

- Observed data are sequentially assimilated, thus EnKF is suitable for reservoir monitoring and performance prediction (Nævdal et al. 2002, 2005).

- Both model parameters (e.g. porosity, permeability) and model state variables (e.g. pressure, phase saturation) can be estimated (Gu and Oliver 2005; Lorentzen et al. 2005).

- EnKF provides assessment of uncertainty in reservoir characterization and production predictions as a byproduct of the estimation (Gao et al. 2006; Zafari and Reynolds 2005).

EnKF has been applied to several synthetic cases for parameter estimations or production optimization (Brouwer et al. 2004; Lorentzen et al. 2006; Wang et al. 2007). The parameters that can be estimated, have expanded from porosity, permeability and facies distribution (Liu and Oliver 2005b,a) to water oil contact (Thulin et al. 2007), vertical transmissibility multipliers and fault transmissibilities (Evensen et al. 2007). On the other hand, the applications of EnKF to real field cases in the literature are rare. Haugen et al. (2006) presented a study for a North Sea field, in which EnKF is used for assimilating production data. Evensen et al. (2007) also applied EnKF to a North Sea reservoir. Parameters estimated in their study included permeability, porosity, initial fluid contacts, vertical transmissivity multipliers and fault transmissivity multipliers. Bianco et al. (2007) applied EnKF to a saturated oil reservoir and investigated the influence of ensemble size on the history matching results. In this paper, we apply EnKF with hierarchical parameters in a fairly large deepwater reservoir for which the trend in the property field is unknown, and for which there is also a large uncertain related to the variogram range.

In the following sections, the methodology is presented followed by the analysis and discussion of the results from the field application. We also make a qualitative comparison among the results obtained from EnKF with double stochastic hierarchical model (Hierarchical EnKF), standard EnKF and traditional manual history matching.

Methodology

Double stochastic hierarchical parameters In history matching, trends are usually considered as deterministic features and heterogeneities are treated as stochastic correlated features, the concept of which is known as universal kriging in geostatistics. The universal kriging theory, however, does not allow for any uncertainty in the trend (or drift) model. Omre (1987) proposed the Bayesian kriging which is a combination of Bayesian theory and kriging technique. Bayesian kriging allows quantifying the uncertainty associated with the estimation of geostatistical parameters. Applying the ideas similar to Bayesian kriging, we propose the method of hierarchical stochastic model with ensemble Kalman filter for history matching. Two important differences between Bayesian kriging and our proposed method are emphasized. First, kriging theory requires exact data, thus, no measurement errors are applied in the estimating process using Bayesian kriging; small measurement errors, however, are added to the geo-data, when using EnKF to estimate geostatistical parameters. Second, the data that Bayesian kriging uses should be linearly related to the estimation points, since kriging is a linear estimator; but, EnKF is fairly robust to nonlinearity in relationships, thus, the dynamic production data can be sequentially assimilated to update the estimation of geostatistical parameters. The results of a field study shows that the influence of production data on the estimation of geostatistical parameters is quite significant. A detail discussion of the results is given in the later section of field application.

The stochastic hierarchial model provides a way of treating both heterogeneities and trends as stochastic features for history matching. Here, the trends we are referring to are not the large-scale trends related to long-term changes of sediment environment, since they can be determined well from geological knowledge and seismic data, but the regional trends in permeability or porosity that are difficult to identify in data. For practical modeling, the conditioning well data for estimating trends are usually sparse and regional trends are only reproduced in the neighborhood of wells, so the variance or uncertainty existing in the regional trends should be considered. Thus, we propose to use a double stochastic hierarchical model for generating porosity and/or logarithm of permeability fields.

Because the variability in the hierarchical method will be quite large, it is useful to transform the property field to maintain the values of physical variables within plausible limits. In this paper, we use $\mathbf{\Psi_T}$ to denote the variable fields before being transformed, correspondingly $\mathbf{\Psi}$ stands for reservoir properties in real scale. We will talk about the transformation in a later subsection. In the hierarchical model, $\mathbf{\Psi_T}$ are expressed as the sum of a relative large scale trend, $\mathbf{\Theta}$, and a small scale heterogeneity or fluctuation, $\mathbf{U}$.

$$\mathbf{\Psi_T} = \mathbf{\Theta} + \mathbf{U}\,, \tag{1}$$

Polynomial trend model In this model of uncertainty, the small scale features $\mathbf{U}$ might be represented as Gaussian random fields, while the large scale trends $\mathbf{\Theta}$ in the properties might be represented through polynomial functions of position with uncertain coefficients. If, for example, we wish to include linear and quadratic trends in the reservoir model, then we might write,

$$\Theta = c_1 m + c_2 x + c_3 y + c_4 x^2 + c_5 y^2 + c_6 xy\,, \tag{2}$$

where c_1 to c_6 are random coefficients. Eq. 3 shows how the 2D trend is formed using a quadratic polynomial equation with six coefficients.

$$\begin{bmatrix} \Theta_1 \\ \vdots \\ \Theta_{N_g} \end{bmatrix} = \begin{bmatrix} m & \frac{i_1}{n_x} - \frac{1}{2} & \frac{j_1}{n_y} - \frac{1}{2} & (\frac{i_1}{n_x} - \frac{1}{2})^2 & (\frac{j_1}{n_y} - \frac{1}{2})^2 & (\frac{i_1}{n_x} - \frac{1}{2})(\frac{j_1}{n_y} - \frac{1}{2}) \\ \vdots & \vdots & \vdots & \vdots & \vdots & \vdots \\ m & \frac{i_{N_g}}{n_x} - \frac{1}{2} & \frac{j_{N_g}}{n_y} - \frac{1}{2} & (\frac{i_{N_g}}{n_x} - \frac{1}{2})^2 & (\frac{j_{N_g}}{n_y} - \frac{1}{2})^2 & (\frac{i_{N_g}}{n_x} - \frac{1}{2})(\frac{j_{N_g}}{n_y} - \frac{1}{2}) \end{bmatrix} \begin{bmatrix} c_1 \\ c_2 \\ c_3 \\ c_4 \\ c_5 \\ c_6 \end{bmatrix}, \tag{3}$$

where i, j are the coordinate indices, n_x is the number of grids in $x-$direction and n_y is the number of grids in $y-$direction. N_g represents the number of gridblocks in one layer. Eq. 3 can be expressed in a concise form as

$$\mathbf{\Theta} = \mathbf{\Theta_p}\mathbf{\Theta_c}\,, \tag{4}$$

In Eq. 4, $\mathbf{\Theta}$ represents the column vector on the left hand side of Eq. 3; $\mathbf{\Theta_p}$ is the deterministic trend basis matrix and $\mathbf{\Theta_c}$ is the column vector of trend coefficients. The trend pattern matrix $\mathbf{\Theta_p}$ is composed of power and cross product terms of the Cartesian coordinates. In particular, the first column of matrix $\mathbf{\Theta_p}$ contains the transformed uniform mean m of reservoir property field (transformation is achieved using Eq. 6). By multiplying a random trend coefficient c_1, we can adjust the property mean among ensemble. Different values of c_1 may be applied for the reservoir with multiple layers having variation in the properties among different layers. Moreover, different reservoir properties should be applied with different values of c_1 because of their different scales, such as porosity and log permeability. All the trend coefficients are generated from the normal distribution. The stochastic linear and nonlinear terms together in the polynomial trend model can simulate very diverse trends. In the field application section, we show two trend maps of porosity and log permeability (Fig. 4). In practical modeling, it may not be necessary to use all six terms, or it may be desirable to include other trends according to need.

Heterogeneity Heterogeneities or fluctuations are spatially correlated stochastic features. The correlation of these features either can be expressed by a covariance or by a variogram model. Although variogram estimation is critical to the generation of geostatistical realizations, a reliable variogram model is not easy to infer from sparse data, thus, there is unavoidable uncertainty in the variogram model. In such a case, the spatial variogram parameters such as correlation length, may be treated as a stochastic variable. In practice, what type of distribution should be applied depends on the available information. Pardo-Igúzquiza (1999) used Bayesian inference to study spatial covariance parameters with different prior distributions, such as trapezoidal, uniform and several triangular distributions. A valid quantification of uncertainty existing in the variogram results in a better description of heterogeneity fields.

Transformation of hierarchical parameters When variability due to uncertainty trends is added to the random variable, the need for a transformation is necessary. The reason is that when the sum of heterogeneity and the trend is calculated under real scale, the large variability can cause non-physical values. One standard approach to solve this problem is truncation of extreme values of the parameters. But by doing so, the histogram of generated reservoir properties may have two peaks at two extreme ends in addition to a peak near the mean, in which case the benefits of using the double stochastic model is substantially reduced. Thus, a transformation equation that not only can maintain a physical meaning to the generated reservoir property fields, but also reduces the negative effect of truncation can be used. The formula that we use for transforming reservoir properties from transformed scale to real scale is given in Eq. 5.

$$\mathbf{\Psi} = \frac{\Psi_{max}\exp(\mathbf{\Psi_T}) + \Psi_{min}}{1+\exp(\mathbf{\Psi_T})}\,, \tag{5}$$

where Ψ_{max} and Ψ_{min} are the maximum and minimum plausible values of porosity or logarithm permeability. Note that in Eq. 5, as $\mathbf{\Psi_T} \to -\infty$, $\mathbf{\Psi} \to \mathbf{\Psi_{min}}$ and as $\mathbf{\Psi_T} \to \infty$, $\mathbf{\Psi} \to \mathbf{\Psi_{max}}$. The transformation is more clear if one instead considers Eq. 6, the back-transformation of Eq. 5,

$$\mathbf{\Psi_T} = \log\left[\frac{\mathbf{\Psi} - \Psi_{min}}{\Psi_{max} - \mathbf{\Psi}}\right]. \tag{6}$$

EnKF with double stochastic hierarchical parameters Instead of limiting the double stochastic hierarchical model to generation of the initial ensemble, we include the hierarchical parameters into the state vector, replacing porosity and permeability that are usually used in EnKF. Thus, during the history matching process, instead of updating porosity and permeability directly, their two different scale components: the small-scale heterogeneity of each gridblock and the large-scale trend coefficients of each layer in a reservoir are updated. Continually updating the large scale parameters (trend coefficients) can effectively enhance the influence of EnKF during updating. Moreover, as mentioned before, determining trends in reservoir depends on data, but the fact is that static well data are usually limited and sparse, and that wells are preferentially drilled in regions of good reservoir properties. Thus, if only static data are used for estimating trends, there is possibility of being misled by generating reservoir property fields that are too optimistic. On the other hand, when production data are used for estimating trends, we may get rid of these pitfalls when only static data are used. Because the procedure is slightly different from standard EnKF, we have included some details.

Generation of initial ensemble Application of EnKF begins with the generation of N_e unconditional realizations of $\mathbf{U}$ and $\mathbf{\Theta_c}$. The initial unconditional ensemble, $\mathbf{Y_0^f}$, is a collection of random initial state vectors:

$$\mathbf{Y_0^f} = [\mathbf{y_{0\,1}^f}, \mathbf{y_{0\,2}^f}, \cdots, \mathbf{y_{0\,N_e}^f}]\,, \tag{7}$$

where each state vector contains the heterogeneity and the trend coefficients.

$$\mathbf{y_{0\,j}^f} = \begin{bmatrix} \mathbf{U_j} \\ \mathbf{\Theta_{c\,j}} \end{bmatrix} = \begin{bmatrix} U_{\phi_1,j} \\ \vdots \\ U_{\phi_{N_g},j} \\ U_{ln\kappa_1,j} \\ \vdots \\ U_{ln\kappa_{N_g},j} \\ c_{1_\phi,j} \\ c_{1_{ln\kappa},j} \\ c_{2,j} \\ \vdots \\ c_{6,j} \end{bmatrix}, \tag{8}$$

and the subscript 0 denotes initial condition.

If we have some prior knowledge about the reservoir, for example, well logs, the next step is to assimilate such static well data. Thus, each realization is updated with the following data assimilation equation:

$$\mathbf{y_{0\,j}^u} = \mathbf{y_{0\,j}^f} + \mathbf{K_{e\,0}}(\mathbf{d_{obs\,j}} - \mathbf{H}\mathbf{\Psi_{T\,j}})\,. \tag{9}$$

The superscript u stands for updated, $\mathbf{K_{e\,0}}$ is the Kalman gain, and $\mathbf{H}$ is the observation operator whose components have value 1 at well locations and 0 elsewhere. $\mathbf{\Psi_{T\,j}}$ is the reservoir property vector before being transformed. The calculation of $\mathbf{\Psi_{T\,j}}$ was discussed in the previous section. $\mathbf{d_{obs\,j}}$ is the observation vector that was obtained by adding perturbations to the transformed static well data. The transformation was achieved using Eq. 6 and the perturbations are sampled from a Gaussian distribution with mean 0 and small standard deviations. Finally, we get the conditional or updated initial ensemble $\mathbf{Y_0^u}$:

$$\mathbf{Y_0^u} = [\mathbf{y_{0\,1}^u}, \mathbf{y_{0\,2}^u}, \cdots, \mathbf{y_{0\,Ne}^u}], \tag{10}$$

Assimilating production data In order to continually update the estimates of $\mathbf{U}$ and $\mathbf{\Theta_c}$, the next step is sequentially assimilating production data whenever they are available. In this sequential data assimilation process, along with $\mathbf{U}$ and $\mathbf{\Theta_c}$, three additional dynamic variables, pressure $\mathbf{P}$, water saturation $\mathbf{S_w}$ and gas saturation $\mathbf{S_g}$ (if three-phase flow model) are included into the state vector. Eq. 11 shows that the updated state vector of each realization is obtained as a combination of forecast state vector and innovation term that is a linear function of perturbed observation vector $\mathbf{d_{obs\,k,j}}$ and predicted data vector $\mathbf{d_{k,j}}$.

$$\mathbf{y_{k\,j}^u} = \begin{bmatrix} \mathbf{U} \\ \mathbf{\Theta_c} \\ \mathbf{P} \\ \mathbf{S_w} \\ \mathbf{S_g} \end{bmatrix}_j^u = \begin{bmatrix} \mathbf{U} \\ \mathbf{\Theta_c} \\ \mathbf{P} \\ \mathbf{S_w} \\ \mathbf{S_g} \end{bmatrix}_j^f + \mathbf{K_{ek}}(\mathbf{d_{obs\,k,j}} - \mathbf{d_{k,j}}), \tag{11}$$

where the subscript k is the time index. Kalman gain $\mathbf{K_{ek}}$ can be calculated using the following equation.

$$\mathbf{K_{ek}} = \mathbf{C_{Y\,k}^f H_k^T (H_k C_{Y\,k}^f H_k^T + C_{D\,k})^{-1}}, \tag{12}$$

where $\mathbf{C_{D\,k}}$ is the covariance matrix for the observation. $\mathbf{C_{Y\,k}^f}$ is the covariance matrix for the ensemble, which is calculated using Eq. 13.

$$\mathbf{C_{Y\,k}^f} = \frac{\mathbf{1}}{\mathbf{N_e - 1}}(\mathbf{Y_k^f} - \overline{\mathbf{Y}}_\mathbf{k}^\mathbf{f})(\mathbf{Y_k^f} - \overline{\mathbf{Y}}_\mathbf{k}^\mathbf{f})^\mathbf{T}, \tag{13}$$

where $\overline{\mathbf{Y}}_\mathbf{k}^\mathbf{f}$ is the mean of the ensemble of state vectors.

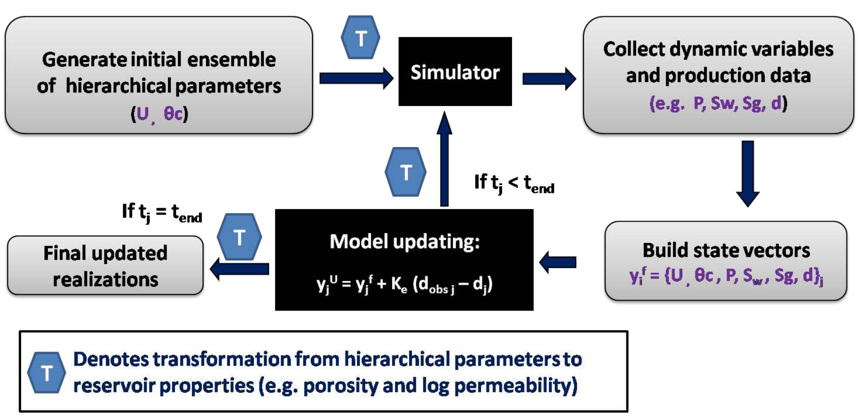

Figure 1: Flowchart of EnKF with hierarchical parameters

The algorithm given above is for standard EnKF in combination with the double stochastic hierarchical model. A flow chart of this procedure is provided in Fig. 1. The hierarchical stochastic model can also be easily combined with any iterative schemes of EnKF (Zafari et al. 2006; Gu and Oliver 2007) for more effectively solving highly nonlinear problems. The primary extra computation cost of using the stochastic hierarchical model is the transformation of converting hierarchical parameters to reservoir properties, but such cost is negligible compared to the cost of numerical flow simulation or matrix computation.

Application on a deepwater reservoir

Description of field and simulation model The deepwater reservoir PFJ2 is located in the Gulf of Mexico. There are 3 aquifers, 2 water injection wells and 6 production wells in the field. The production wells came online at different times during the production history. Fig. 2 shows the structure of PFJ2. The reservoir simulation model is an Eclipse 100 black oil model (Schlumberger 2007) with grid dimensions of 159 × 149 × 5. The total number of cells is 118,455, of which 95,379 are active. The horizontal grid has a resolution of 164 ft × 164 ft. There are 5 layers with thickness varying between 0.1 ft and 23 ft. The field has been produced for about 6 years. In the simulation model, the production wells were produced by the target oil production rate with minimum bottom hole pressure as the secondary constraint. The injectors were also on rate control with maximum bottom hole pressure as the secondary constraint.

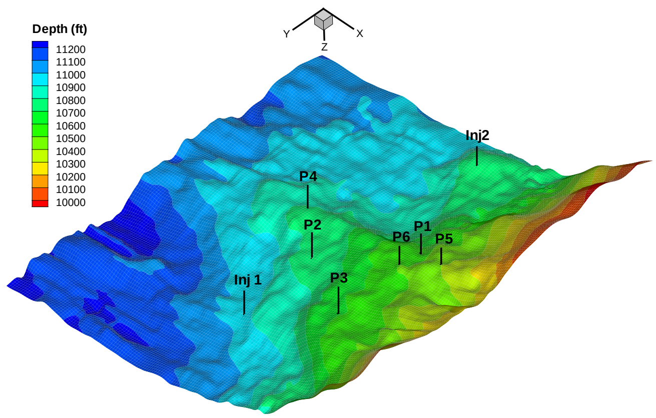

Figure 2: Structure map of PFJ2 field.

Traditional manual history matching and the standard EnKF Traditional manual history matching has previously been applied for this field case. As observed in Fig. 3, manual history matching of the bottom hole pressure of producer P5 was partially accomplished by modifying the transmissibility within a zone surrounding the well, which results in a geologically unrealistic permeability field. In addition, the water cut history of producer P1 and the fluctuating gas oil ratio data can not be easily matched using manual history matching.

Without knowledge of data used to create the model, it is hard to identify which aspects of the model can be altered, so we have to make some reasonable assumptions for applying EnKF. We have assumed that there is no uncertainty in the structural model (e.g. the locations of aquifers etc.) and the fluid contacts. We also assumed that the values of porosity and permeability at the well locations in the reservoir simulation model provided to us are sufficiently accurate to be used as static well data.

Standard EnKF was also used to solve this history matching problem, meaning that the initial ensemble was generated using sequential Gaussian simulation and that the state vector includes porosity, log permeability and dynamic state variables and iteration was not used. The input parameters of sequential Gaussian simulation, such as mean and variogram model are obtained by carrying out statistical analysis of the given simulation model assuming ergodicity. The ensemble size is 60. The data assimilation is carried out approximately every three months and the total number of data assimilation times is 26. The assimilated production data include bottom hole pressure (well constraint), water cut, gas oil ratio, and flow rate target (well control target). The standard EnKF did not give a totally satisfactory history match as shown in Fig. 8. Specifically, none of the realizations were able to predict water breakthrough of P1 by implementing the standard EnKF. Moreover, the ensemble prediction of bottom hole pressure of P5 are generally higher than the observations. Many factors can influence the performance of EnKF, but the primary reason, in this case, is the relatively small variability in the initial reservoir property fields, which limits the adjusting space of EnKF. As we generated the initial ensemble of porosity and permeability based on the given simulation model, it seems that we underestimated the uncertainty existing in the model. In order to solve this uncertainty underestimation problem, we applied the stochastic hierarchical model in combination with EnKF.

Stochastic hierarchical model in combination with EnKF (Hierarchical EnKF) Before assimilating production data, we have prior knowledge of porosity and permeability at 40 well completion locations in the reservoir, which was used for doing geostatistical analysis. But, the limited observations of the reservoir properties results in large uncertainty in correlation length and variogram model. To account for uncertainty in the correlation length, the correlation length used for generating each realization of heterogeneity field with sequential Gaussian simulation is sampled from a uniform distribution with fairly broad limits. By generating correlation length uniformly from the possible range (250 m to 1250 m), the uncertainty introduced by the undetermined correlation length is accounted for. The trend model used in this field study is a polynomial formulation of three terms shown in Eq. 14.

$$\Theta = c_1(m + m_w) + c_2 a_x (x - O_x)^2 + c_3 a_y (y - O_y)^2 \,, \tag{14}$$

where c_1, as mentioned previously, is sampled from a normal distribution with mean 1, m is the transformed mean of reservoir properties, and m_w is a weighting parameter for adjusting the mean when c_2 and c_3 are sampled from a normal distribution with a nonzero mean. a_x and a_y are shape adjusting parameters, and O_x and O_y are the parameters controlling the center of trends. All the parameters shown in Eq. 14 are fixed, except the stochastic trend coefficients c_1, c_2, c_3 that are included into the state vector for further estimating by incorporating the information of production data. An example of the trends used for porosity and log permeability in this application is shown in Fig. 4. Fig. 5 shows four realizations of log permeability fields with differing correlation ranges, which are transformed from their corresponding heterogeneity fields and trend coefficients in the initial ensemble. We compare initial grid standard deviation maps of reservoir properties from Hierarchical EnKF and the standard EnKF in Fig. 6. It is evident that the standard deviations with Hierarchical EnKF are much higher. In the models generated from Hierarchical EnKF, the standard deviation increases significantly as we move away from the drilled region. One important thing to note is that a relatively small ensemble size (40 members) is used for Hierarchical EnKF compared to the standard EnKF where an ensemble of 60 realizations was used.

At first, without assimilating any production data, the initial ensemble was run forward in time from the initial time all the way to the end. Fig. 7 shows the comparison of the predicted production data from forward runs between Hierarchical EnKF and the standard EnKF. Water breakthrough during the production history (the production history ends at day 2032) of P1 was observed using Hierarchical EnKF, whereas the water breakthrough time predicted by the standard EnKF was far away from the actual observations. If the initial ensemble adequately captures the uncertainty, we should expect that the actual data fall within the range of outcomes from the ensemble. Through comparison, the spread of the realizations generated with the hierarchical model gives a better representation of the initial uncertainty in the model forecasts.

We implemented a parallel version of Hierarchical EnKF with multi-processors to continually assimilate the production data using a localization scheme to reduce the spurious correlations and to increase the effective rank of the ensemble (Chen and Oliver 2009; Gaspari and Cohn 1999). The same number of data assimilation timesteps and assimilated production data were used for implementing Hierarchical EnKF as for the standard EnKF. The predictions during history matching process from Hierarchical EnKF are compared with that from the standard EnKF and are shown in Fig. 8. The water cut data of P1 can not be matched by implementing the standard EnKF while Hierarchical EnKF gave a reasonable match to the water cut data. For the water cut data of other wells, Hierarchical EnKF resulted in a better match to the water breakthrough time, compared to the standard EnKF. For bottom hole pressure data, both methods gave a good match, but WBHP of P5 and WBHP of P3 got a better match using Hierarchical EnKF. For gas oil ratio, Hierarchical EnKF also gave a better match than the standard EnKF.

Fig. 9 shows the initial and final mean porosity and mean logarithm permeability fields and the corresponding final standard deviation maps. The standard deviation of porosity and permeability are substantially reduced around the drilled area. Moreover, the initial and final mean water saturation maps are also given in Fig. 9. Comparing the final water saturation maps from Hierarchical EnKF with that obtained from manual history matching shown in Fig. 3(c), we can clearly observe that the Hierarchical method has resulted in further advance of water fronts from the two injectors to P1 in Fig. 3(c). In this situation, the water saturation distribution from Hierarchical EnKF is better than the distribution from the manually history matched model. Fig. 10 shows the histograms of the initial and final estimates of trend coefficients. We observe a large influence of production data on the estimates of trend coefficients. The uncertainty existing in the trend coefficients is reduced by sequentially assimilating the dynamic production data.

Conclusions

Because of the complexity of the relationships between data and model variables, it is generally difficult to achieve well-by-well manual history matches that are geologically plausible. The field example discussed in this paper shows such a case. EnKF as an assisted history matching method, circumvents these difficulties inherent to the manual process. However when EnKF is applied for history matching, because of the implicit assumption of Gaussianity, Gaussian simulation is often used for generating the initial ensemble of rock properties, which, at the same time, causes a systematic underestimation of the geostatistical uncertainty. We have shown that hierarchical stochastic structure provides a way to increase the variability of reservoir property fields and avoids the overshooting problem by introducing an appropriate transformation to property fields. The results of the field case study show that the ability to match the water cut and other production data was improved by adding uncertainty in trends. Compared to the standard EnKF, Hierarchical EnKF provided better uncertainty quantification. The results also indicated that an improvement in the generation of the initial ensemble and in the variables describing the property fields gave an improved history match with plausible geology.

Acknowledgment

The first author acknowledges financial support from the OU Consortium on Ensemble Methods. The authors would like to thank Chevron for providing the dataset for this study and the permission to publish this paper. The authors also want to acknowledge the donation of multiple licences of ECLIPSE by Schlumberger and computational resources provided by the OU Supercomputing Center for Education and Research.

References

Bianco, A., Cominelli, A., Dovera, L., Naevdal, G., and Valles, B., 2007. History matching and production forecast uncertainty by means of the ensemble Kalman filter: A real field application (SPE 107161). In *EUROPEC/EAGE Conference and Exhibition*.

Brouwer, D. R., Nævdal, G., Jansen, J. D., Vefring, E. H., and van Kruijsdijk, C. P. J. W., 2004. Improved reservoir management through optimal control and continuous model updating (SPE 90149). In *SPE Annual Technical Conference and Exhibition, 26-29 September, Houston, Texas*.

Capen, E. C., 1976. The difficulty of assessing uncertainty. *J. Petroleum Technology*, **28** (8): 843–850.

Chen, Y. and Oliver, D. S., 2009. Application of ensemble-based closed-loop optimization on brugge field (SPE 118926). In *Proceedings of the SPE Reservoir Simulation Symposium*.

Deutsch, C. V., 2002. *Geostatistical Reservoir Modeling*. Oxford, first edition.

Evensen, G., Hove, J., Meisingset, H. C., Reiso, E., Seim, K. S., and Espelid, Ø., 2007. Using the EnKF for assisted history matching of a North Sea reservoir model (SPE 106184). In *Proceedings of the 2007 SPE Reservoir Simulation Symposium,*.

Gao, G., Zafari, M., and Reynolds, A. C., 2006. Quantifying uncertainty for the PUNQ-S3 problem in a Bayesian setting with RML and EnKF. *SPE Journal*, **11** (4): 506–515. doi:10.2118/93324-PA.

Gaspari, G. and Cohn, S. E., 1999. Construction of correlation functions in two and three dimensions. *Quarterly Journal of the Royal Meteorological Society*, **125** (554): 723–757.

Gu, Y. and Oliver, D. S., 2005. History matching of the PUNQ-S3 reservoir model using the ensemble Kalman filter. *SPE Journal*, **10** (2): 51–65. doi:10.2118/89942-PA.

Gu, Y. and Oliver, D. S., 2007. An iterative ensemble Kalman filter for multiphase fluid flow data assimilation. *SPE Journal*, **12** (4): 438–446.

Haugen, V., Natvik, L.-J., Evensen, G., Berg, A., Flornes, K., and Nævdal, G., 2006. History matching using the ensemble Kalman filter on a North Sea field case (SPE 102430). SPE Journal to appear.

Liu, N. and Oliver, D. S., 2005a. Critical evaluation of the ensemble Kalman filter on history matching of geologic facies. *SPE Reservoir Evaluation & Engineering*, **8** (6): 470–477. doi:10.2118/92867-PA.

Liu, N. and Oliver, D. S., 2005b. Ensemble Kalman filter for automatic history matching of geologic facies. *Journal of Petroleum Science and Engineering*, **47** (3–4): 147–161.

Lorentzen, R. J., Berg, A. M., Nævdal, G., and Vefring, E. H., 2006. A new approach for dynamic optimization of waterflooding problems (SPE 99690). In *SPE Intelligent Energy Conference and Exhibition*.

Lorentzen, R. J., Nævdal, G., Vàlles, B., Berg, A. M., and Grimstad, A.-A., 2005. Analysis of the ensemble Kalman filter for estimation of permeability and porosity in reservoir models, (SPE 96375). In *SPE Annual Technical Conference and Exhibition*.

Nævdal, G., Johnsen, L. M., Aanonsen, S. I., and Vefring, E. H., 2005. Reservoir monitoring and continuous model updating using ensemble Kalman filter. *SPE Journal*, **10** (1): 66–74. doi:10.2118/84372-PA.

Nævdal, G., Mannseth, T., and Vefring, E. H., 2002. Near-well reservoir monitoring through ensemble Kalman filter: SPE 75235. In *Proceedings of SPE/DOE Improved Oil Recovery Symposium*.

Oliver, D. S., Reynolds, A. C., and Liu, N., 2008. *Inverse Theory for Petroleum Reservoir Characterization and History Matching*. Cambridge University Press, Cambridge, first edition.

Omre, H., 1987. Bayesian Kriging-merging observations and qualified guesses in Kriging. *Mathematical Geology*, **19** (1): 25–39.

Pardo-Igúzquiza, E., 1999. Bayesian inference of spatial covariance parameters. *Mathematical Geology*, **31** (1): 47–65.

Schlumberger, 2007. ECLIPSE 100 Technical Description 2007A, GeoQuest.

Thulin, K., Li, G., Aanonsen, S. I., and Reynolds, A. C., 2007. Estimation of initial fluid contacts by assimilation of production data with EnKF (SPE 109975). In *Proceedings of the 2007 SPE Annual Technical Conference and Exhibition*.

Wang, C., Li, G., and Reynolds, A. C., 2007. Production optimization in closed-loop reservoir management, SPE 109805. In *Proceedings of the SPE Annual Technical Conference and Exhibition, 11-14 November 2007, Anaheim, California*.

Yang, K., Tan, K. S., Kramer, K., and Yarus, J. M., 2000. Stochastic 3D geological modeling of deep water reservoir: Methodology and case studies. *Gulf Coast Association of Geological Societies Transactions*, **L**: 463–472.

Zafari, M., Li, G., and Reynolds, A. C., 2006. Iterative forms of the ensemble Kalman filter. In *Proceedings of the 10th European Conference on the Mathematics of Oil Recovery — Amsterdam*, A030.

Zafari, M. and Reynolds, A. C., 2005. Assessing the uncertainty in reservoir description and performance predictions with the ensemble Kalman filter (SPE 95750). In *Proceedings of the SPE Annual Technical Conference and Exhibition*.

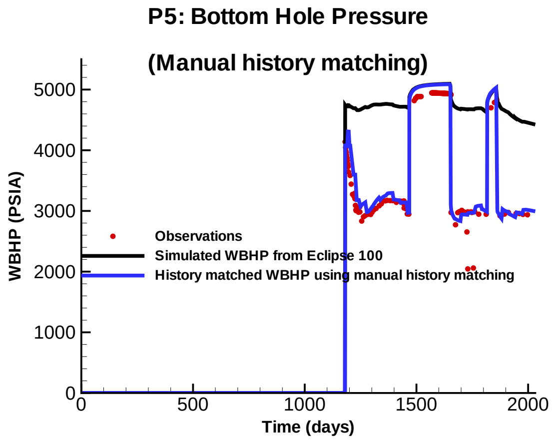

(a) P5: Bottom hole pressure

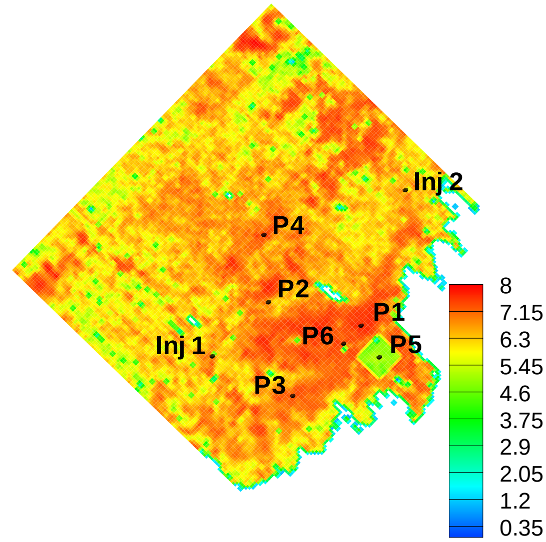

(b) History matched permeability of model layer 1

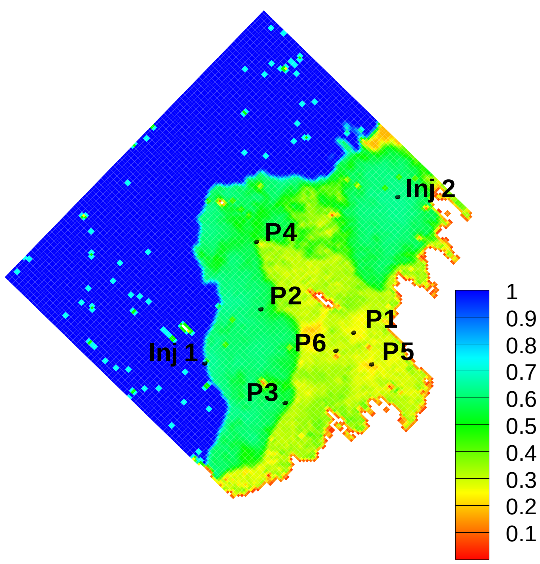

(c) Final water saturation of model layer 1

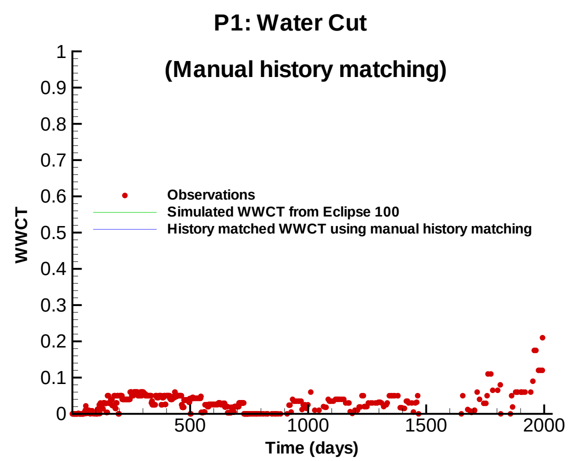

(d) P1: Water cut

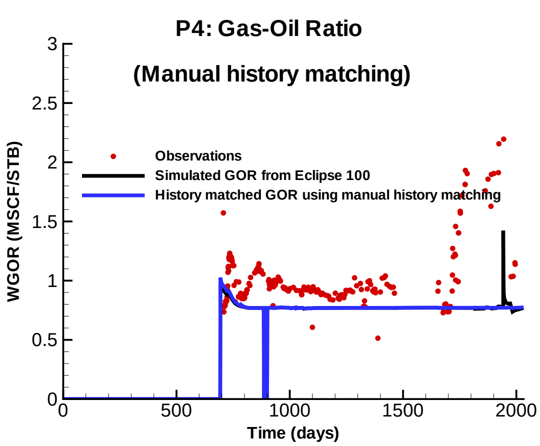

(e) P4: Gas-oil ratio

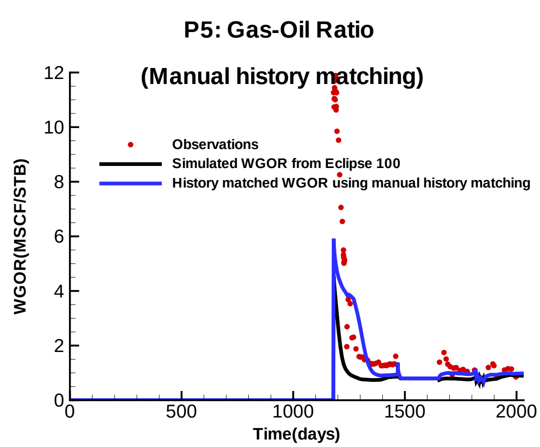

(f) P5: Gas-oil ratio

Figure 3: Traditional manual history matching results

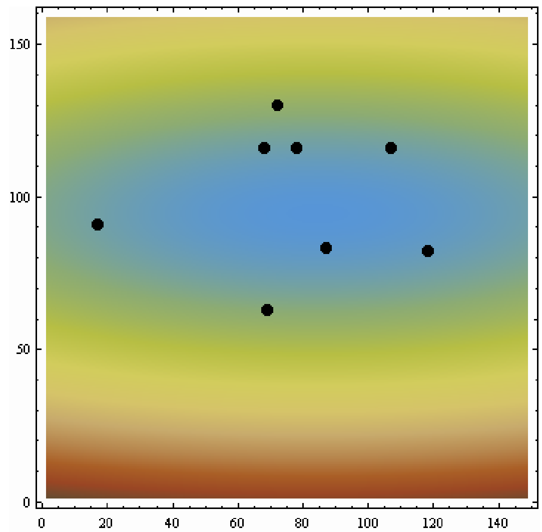

(a) Permeability

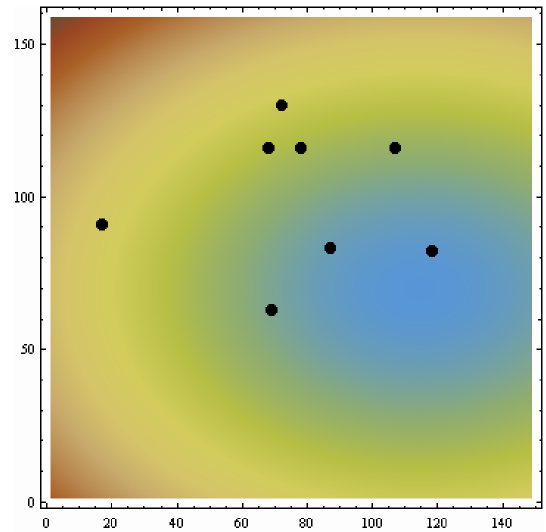

(b) Porosity

Figure 4: An example of trend maps (from warm color to cold color, value increases).

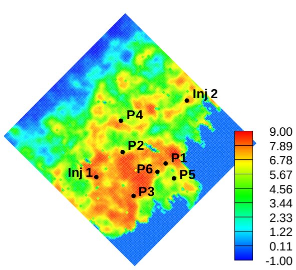

(a) Realization 1

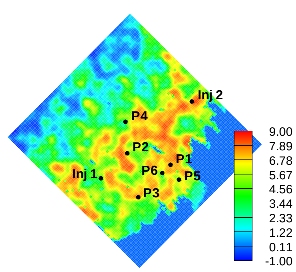

(b) Realization 2

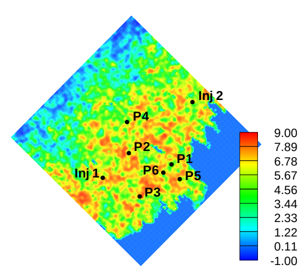

(c) Realization 3

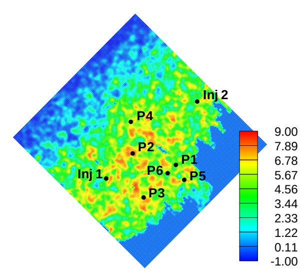

(d) Realization 4

Figure 5: Four initial realizations of log permeability showing variability in correlation length of heterogeneity.

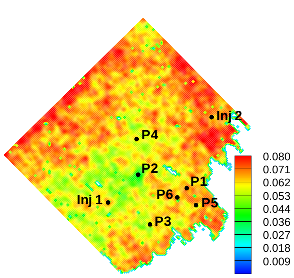

(a) STD of ϕ (HE)

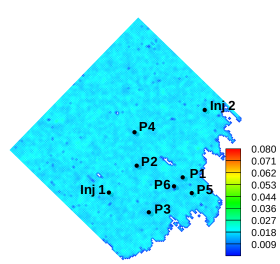

(b) STD of ϕ (SGSIM)

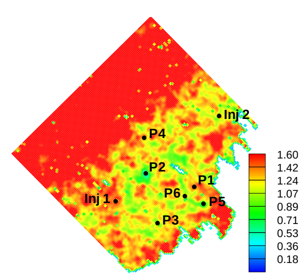

(c) STD of $Ln\kappa_H$ (HE)

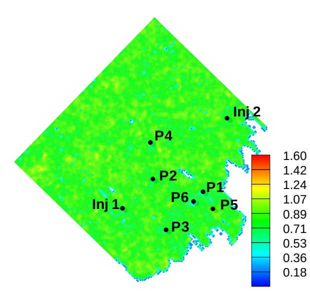

(d) STD of $Ln\kappa_H$ (CoSGSIM)

Figure 6: Standard deviation of porosity and log permeability in model layer 1. ϕ stands for porosity and $Ln\kappa_H$ stands for logarithm horizontal permeability. HE denotes Hierarchical EnKF, SGSIM denotes sequential Gaussian simulation and Co-SGSIM denotes sequential Gaussian co-simulation.

Hierarchical EnKF

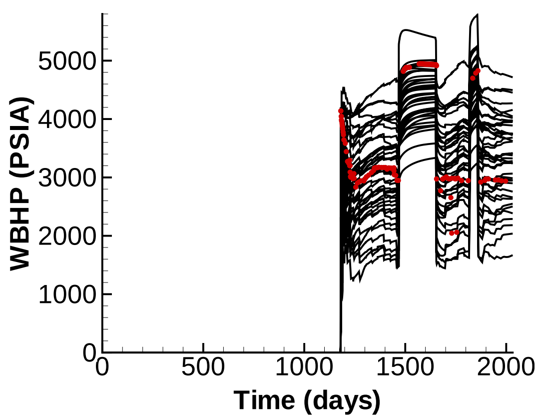

P5: Bottom hole pressure

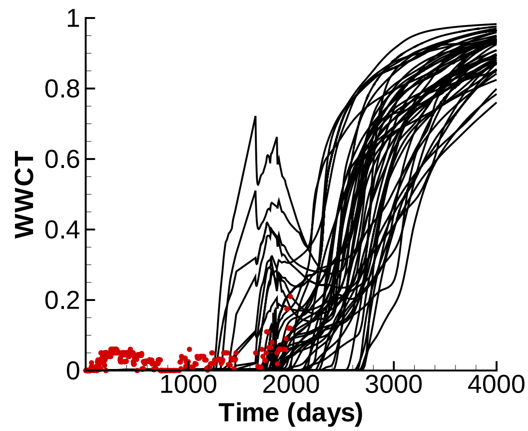

P1: Water cut

SGSIM

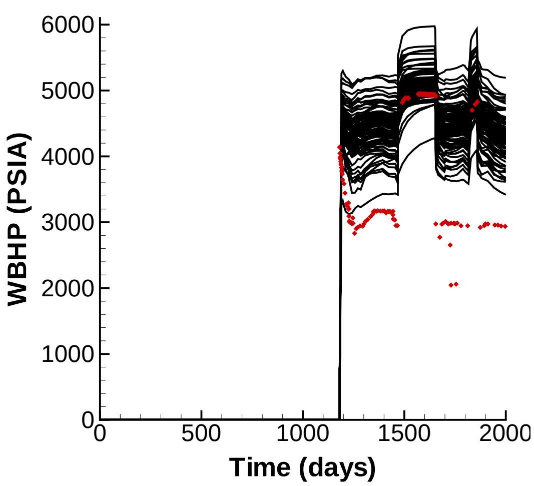

P5: Bottom hole pressure

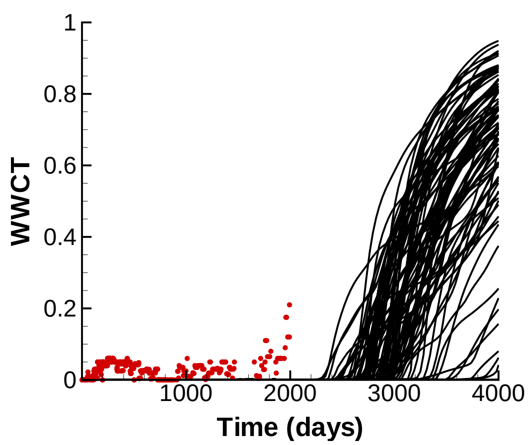

P1: Water cut

Figure 7: The production forecast based on the initial ensembles of porosity and permeability (black lines), and the observations (red dots).

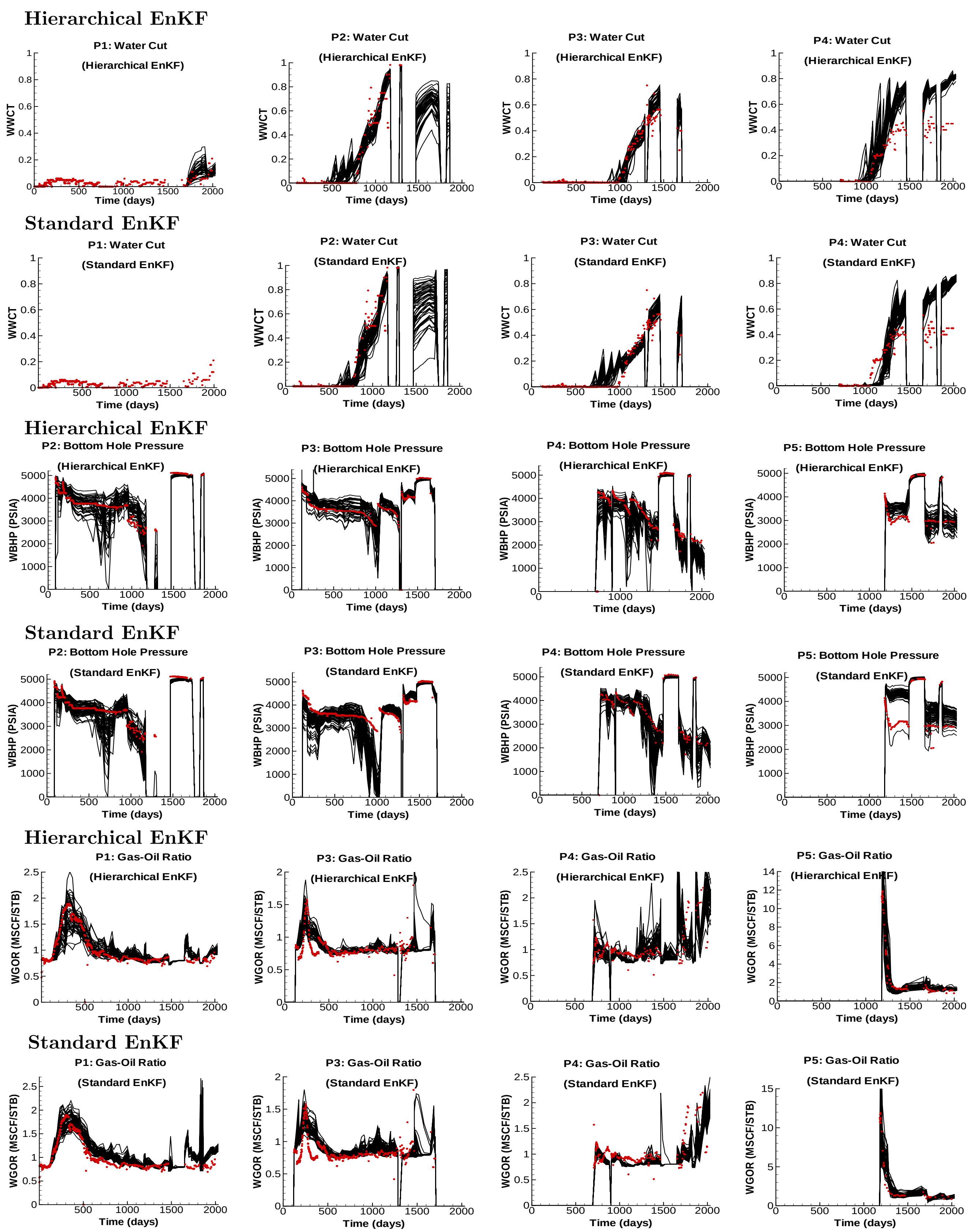

Figure 8: The production data during the history matching process and prediction using Hierarchical EnKF and the standard EnKF. (The black lines denote the results from different ensemble members and the red dots denote observations.)

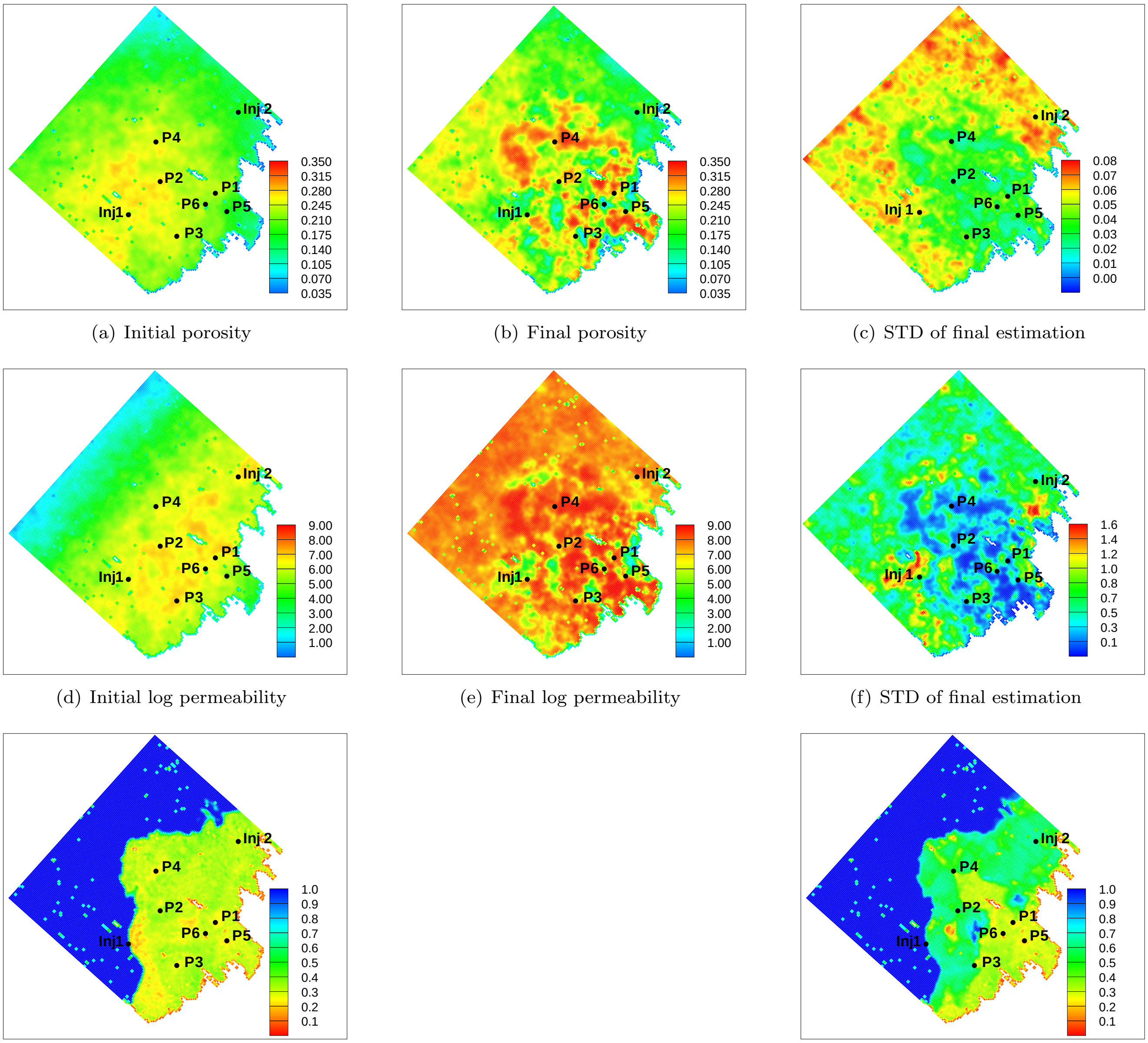

(a) Initial porosity

(b) Final porosity

(c) STD of final estimation

(d) Initial log permeability

(e) Final log permeability

(f) STD of final estimation

(g) Initial water saturation

(h) Final water saturation

Figure 9: Initial and final estimations of porosity and log permeability, the standard deviation of final estimations, and the evolution of water saturation of model layer 1.

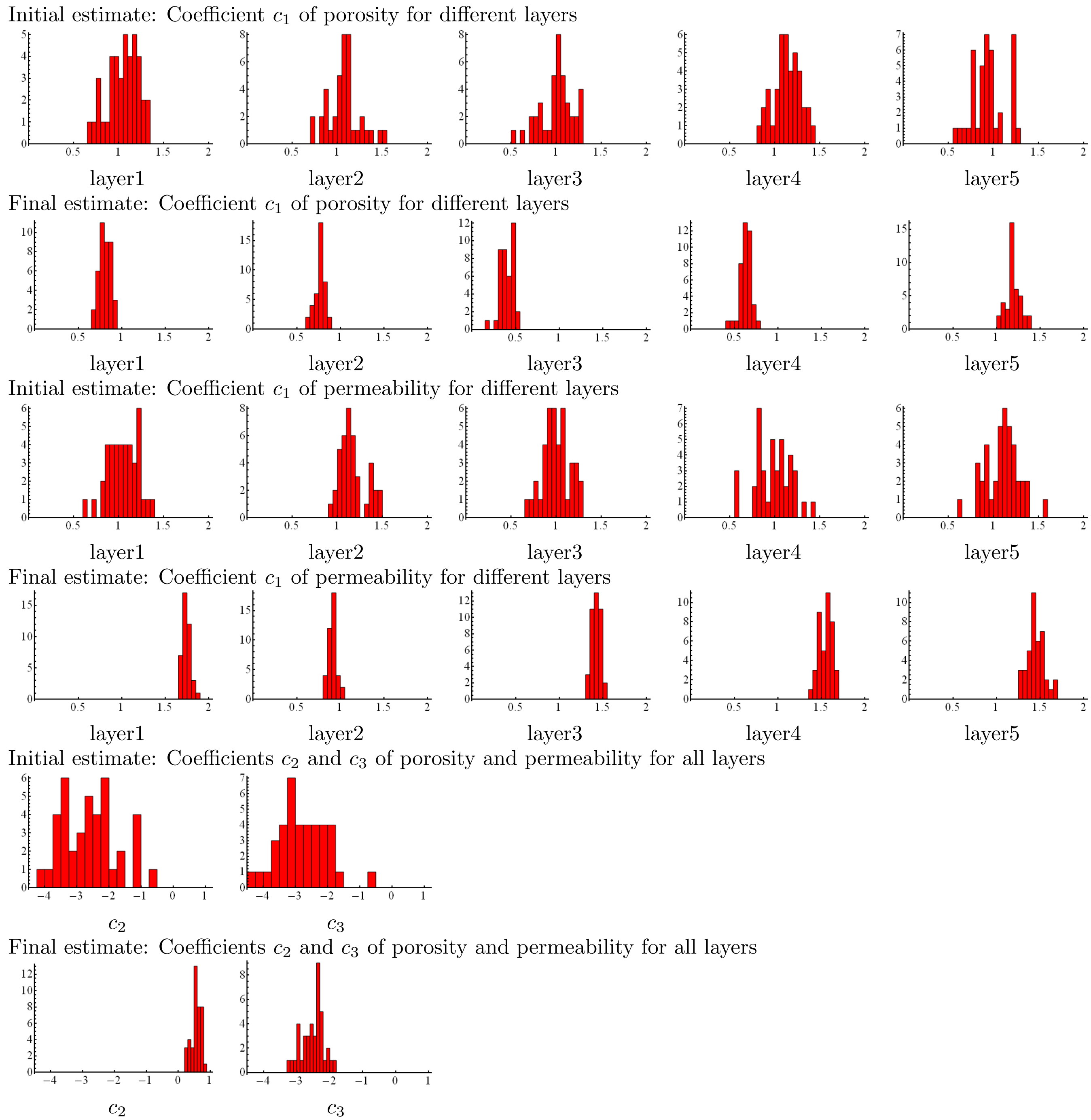

Figure 10: Histograms of trend coefficients.